Diffusion in a one-dimensional bosonic lattice gas

1995 J. Phys. A: Math. Gen. 28 923

(http://iopscience.iop.org/0305-4470/28/4/017)

J. Phys. A: Math. Gen. 28 (1995) 923–940. Printed in the UK

Diffusion in a one-dimensional bosonic lattice gas

Ryszard Kutner†§, Klaus W Kehr‡, Wolfgang Renz‡‖ and Radosław Przeniosło†

† Department of Physics, Warsaw University, Hoża 69, PL-00-681 Warsaw, Poland
‡ Institut für Festkörperforschung, Forschungszentrum Jülich GmbH, Postfach 1913, D-52425 Jülich, Germany

Received 2 August 1994, in final form 5 December 1994

Abstract. A one-dimensional lattice-gas model with order preservation is considered where the occupation probabilities of sites correspond to Bose statistics as a consequence of the prescribed dynamics. The master equation for the particle-cluster dynamics at the sites is formulated. The corresponding continuum nonlinear diffusion equation is derived for the space- and time-dependent concentration fluctuations. The equation can be regarded, in the presence of a drift force, as the Burgers equation when terms irrelevant in the sense of renormalization-group ideas are neglected. Collective centre-of-mass and tagged-particle diffusion are investigated by numerical simulations and the results agree with the analytical derivations. Subdiffusive behaviour of the mean-square displacement of tagged particles and normal collective and centre-of-mass diffusion are observed when no bias is present. The dispersion of the centre-of-mass displacement exhibits superdiffusive behaviour in the case of mean drift of the particles. Discrepancies of about 20% between the numerically determined superdiffusion coefficients and the predictions of the mode-coupling theory are found and discussed.

1. Introduction

In this paper we study a non-interacting one-dimensional *lattice-gas* model with an *order preservation* of particles where *multiple* occupancy of the sites is *not* excluded. The dynamics of this model are constructed in such a way that the equilibrium occupation probabilities of the sites are given by the expression for Bose particles [1]. The exclusion of particle permutations within this one-dimensional model then leads to non-trivial slowed diffusion processes.

There are several reasons why this model has been studied. First, this model exhibits very interesting diffusional behaviour—besides normal collective diffusion in the absence of a bias, anomalous diffusion appears when a uniform bias field is applied, as will be demonstrated below. In this model, the diffusion coefficients and the drift velocities become particle-concentration-dependent. The non-trivial concentration dependence of the collective diffusion coefficient is in contrast to the corresponding result for site-exclusion lattice-gas models. Second, the model is related to the 'repton' model for polymer diffusion [2] (which is a discretized version of the reptation model), where several segments can be accumulated at one site. Third, the model may have a direct application to the transport of particles in disordered (e.g. porous) materials ([3] and references therein) where several particles

§ Present address: Universität Konstanz, Fakultät für Physik, Postfach 5560, D-78434 Konstanz, Germany.
‖ Permanent address: Department of Electrical Engineering and Computer Science, FH Hamburg, Berliner Tor 3, D-20099 Hamburg, Germany.

0305-4470/95/040923+18$19.50

may occupy the same region and when release of the particles is through a one-particle bottleneck.

In section 2 we introduce the model by its master equation and describe a special implementation for numerical simulations. Section 3 describes the derivation of a Burgers equation for the model and its consequences. In section 4 the diffusion of particles in this model is studied when no bias field is present and in section 5 the extension to diffusion under the influence of a bias field is made. Section 6 contains concluding remarks.

2. The master equation of the model

We consider a linear chain with sites numbered by l and with periodic boundary conditions. Particles are randomly occupying the sites of the chain; *multiple* occupancy of the sites is allowed. At each lattice site along the chain an arbitrary number of particles can be piled up, entering and leaving only at the bottom and the top of the piles, then respectively going either to the left or right nearest-neighbour piles with certain probabilities (cf figure 1). Since particles below the top and above the bottom of the piles are immobilized the resulting diffusion process will be slowed down the higher the piles are.

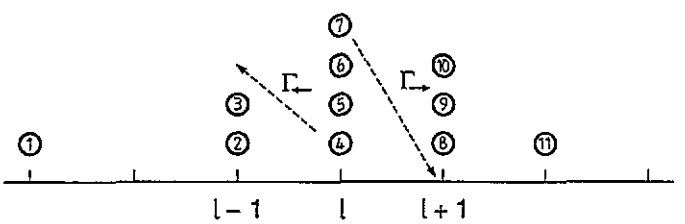

Figure 1. Schematic representation of the one-dimensional bosonic lattice-gas model with order preservation. The possible transitions of the cluster at site l to neighbour sites are indicated.

Let $P_n(l,t)$ be the probability that site l is occupied by n particles at time t and let $P_n(l,l',t)$ be the joint probability that site l is occupied by n particles *and* that site l' is occupied by at least one particle, at time t. We postulate the following master equation for $P_n(l,t)$ $(n = 1, 2, \ldots)$:

$$\frac{\partial P_n(l,t)}{\partial t} = \Gamma_{\leftarrow} P_{n-1}(l, l+1, t) + \Gamma_{\rightarrow} P_{n-1}(l, l-1, t) + (\Gamma_{\leftarrow} + \Gamma_{\rightarrow}) P_{n+1}(l,t) - \Gamma_{\leftarrow} P_n(l, l+1, t) - \Gamma_{\rightarrow} P_n(l, l-1, t) - (\Gamma_{\leftarrow} + \Gamma_{\rightarrow}) P_n(l,t). \tag{1}$$

The master equation (1) describes essentially the dynamics of particle clusters at the sites l where the clusters can grow or shrink by a single-particle transfer. Here $\Gamma_{\rightarrow}$ is the transition rate of a particle in the direction of increasing l and $\Gamma_{\leftarrow}$ the transition rate when l is decreasing. The equation for the probability of no occupancy $P_0(l,t)$ is slightly simpler and can be obtained from (1) by summation over n,

$$\frac{\partial P_0(l,t)}{\partial t} = (\Gamma_{\rightarrow} + \Gamma_{\leftarrow}) P_1(l,t) - \Gamma_{\leftarrow} P_0(l, l+1, t) - \Gamma_{\rightarrow} P_0(l, l-1, t). \tag{2}$$

The probabilities obey the following normalization conditions:

$$\sum_{n=0}^{\infty} P_n(l,t) = 1 \tag{3}$$

and

$$\sum_{n=0}^{\infty} P_n(l', l, t) = P(l, t) = 1 - P_0(l, t) \tag{4}$$

where $P(l, t)$ denotes the probability that at least one particle is present at site l at time t.

We now point out the difference between the model considered here and the standard model of independently diffusing particles. Let us consider the last term of (1). It describes shrinking of the cluster of n particles at site l by a single-particle transition to the left or to the right. The summary rate of departing of a particle from this cluster is $\Gamma_{\leftarrow} + \Gamma_{\rightarrow}$, *independent* of the number $n > 0$ of particles present in it. This fact makes the model different from an ensemble of hopping independent 'Boltzmann' particles, where the rate of transitions of any one of the individual particles to the neighbour sites would be $\Gamma_{\leftarrow} + \Gamma_{\rightarrow}$, and thus the summary rate for cluster decay would be $n(\Gamma_{\leftarrow} + \Gamma_{\rightarrow})$. The characteristic feature described above can be identified in the other terms as well.

We are interested in the concentration of particles at site l at time t. It is defined by

$$c(l, t) = \sum_{n=1}^{\infty} n P_n(l, t) . \tag{5}$$

The master equation for $c(l, t)$ is derived from (1) and (2) by multiplying by n and subsequent summation using conditions (3) and (4). We have

$$\frac{\partial c(l, t)}{\partial t} = \Gamma_{\leftarrow} P(l + 1, t) + \Gamma_{\rightarrow} P(l - 1, t) - (\Gamma_{\leftarrow} + \Gamma_{\rightarrow}) P(l, t) \tag{6}$$

with $P(l, t)$ defined in (4). Equation (6) demonstrates again that the rate of change of concentration at one site does not depend on the concentrations $c(l', t)$, $l' = l, l \pm 1$, of this and the neighbouring sites, rather it is determined by the probabilities $P(l', t)$.

The *stationary* solution of (1) and (2) is easily obtained when the factorization $P_n(l, l') = P_n(l)[1 - P_0(l')]$ is assumed. By iterative solution of the equations we find a distribution

$$P_n(l) = P_0(l)[1 - P_0(l)]^n \qquad n = 0, 1, 2, \ldots . \tag{7}$$

This solution satisfies the normalization condition (3). Since the stationary solution of (1) and (2) is unique, the factorization has been justified. Equation (7) also follows from the combinatorial consideration of distributing N_p indistinguishable 'Bose' particles over N sites. Thus we have shown the equivalence of a classical lattice gas with order preservation and the quantum-mechanical lattice gas.

From equation (7) follows that, using (5), the probability $P(l)$ of having at least one particle present at site l is

$$P(l) = \frac{c(l)}{1 + c(l)} . \tag{8}$$

The stationary occupation probabilities are then given by

$$P_n(l) = \frac{1}{1 + c(l)} \left[\frac{c(l)}{1 + c(l)} \right]^n . \tag{9}$$

Detailed balance conditions for the equilibrium states are easily deduced from (1) and (2) in the form

$$\Gamma_{\rightarrow} P_{n+1}(l) = \Gamma_{\leftarrow} P_n(l)[1 - P_0(l + 1)] \tag{10}$$

for any pair of neighbouring sites l and $l + 1$.

The results described so far are valid for homogeneous systems with $c(l) = \bar{c}$, as well as for disordered systems with spatially varying transition rates and hence space-dependent $c(l)$. The latter case will not be considered further in this paper. A spatially inhomogeneous system with $\Gamma_{\rightarrow} \neq \Gamma_{\leftarrow}$ and reflecting boundary conditions at one end has been considered in [1]. There a Bose distribution for $c(l)$ was obtained. Analogous models of fermionic lattice gases were studied in [4].

We now describe the actual implementation of the kinetic model for particle transport, as defined by the master equation (1), in a direct numerical simulation. We use *periodic* boundary conditions in this paper. We prepare an average, homogeneous concentration $\bar{c}$ of particles in our system both in equilibrium and in the stationary state where we use (8) and (9) for N_p particles distributed over N sites with $c(l) = \bar{c} = N_p/N$. The process of putting particles on the sites of the lattice with a given *average* concentration corresponds to the use of the grand-canonical ensemble for the preparation. Consequently, the actual concentrations deviate slightly (3% or less) from the nominal concentrations, which are always indicated. Random selection of single particles for attempted transitions to neighbouring sites is equivalent to a Poisson process when $N_p \gg 1$ [5]. As discussed above, the transition rates describe cluster growth or shrinkage; a particle in a cluster of size n should then have a rate $\Gamma_{\rightarrow}/n$, or $\Gamma_{\leftarrow}/n$, respectively, for transition to a neighbouring site. An alternative way of implementing the model consists of numbering the particles along the line and in the clusters as shown in figure 1, and preserving the order of the particles during the transitions. Explicitly, a particle at the bottom of a cluster can make a transition with rate $\Gamma_{\leftarrow}$ to the top of the left cluster, a particle on the top of the cluster can perform a transition with rate $\Gamma_{\rightarrow}$, which then leads to the bottom of the right cluster. No other transitions are allowed. As long as we can disregard the enumeration in the study of quantities such as the collective diffusion coefficient, we will obtain the same results as with the original dynamics. The algorithm outlined above is much more convenient for numerical implementation since the particles are easily enumerated. Further, we can now study the diffusion of tagged particles; this will provide additional interesting information.

The version of our model with the preservation of particle order is similar to the so-called repton model of polymer dynamics [2]. However, in our model zero occupancy of sites can also occur. This has to be excluded in the repton model, because *breaking off* and *gluing* processes of the segments of the polymer are not allowed.

3. Derivation of the Burgers equation

Equation (6) of the preceding section connects the time derivative of the local density of particles at a site to the probability of finding particles at this or neighbouring sites, i.e. the first to the zeroth moment. Hence it is not a closed equation. In this section we shall introduce a closed equation for the local concentration; at the same time we shall consider the system on a more coarse-grained scale by using a continuum description. We assume, as our *basic hypothesis*, the following nonlinear relation between $P(l, t)$ and $c(l, t)$:

$$P(l, t) = \frac{c(l, t)}{1 + c(l, t)} . \tag{11}$$

This is a generalization of (8) for non-equilibrium situations, and we expect it to be valid at least close to equilibrium or close to stationary states.

By expanding $P(l, t)$ in derivatives of $c(x, t)$ up to second order we obtain directly from (6)

$$\frac{\partial c(x,t)}{\partial t} = \frac{\partial}{\partial x}\left\{\frac{D_0}{[1+c(x,t)]^2}\frac{\partial c(x,t)}{\partial x}\right\} - \frac{\partial}{\partial x}\left[\frac{v_0}{1+c(x,t)}c(x,t)\right] \tag{12}$$

where $D_0 = (\Gamma_\rightarrow + \Gamma_\leftarrow)/2$ and $v_0 = \Gamma_\rightarrow - \Gamma_\leftarrow$. The lattice constant has been set to unity; moreover, in our numerical calculations the summary transition rate was taken as $\Gamma_\rightarrow + \Gamma_\leftarrow = 1$.

Equation (12) has the form of a continuity equation and the density current is

$$j(x,t) = -\frac{D_0}{[1+c(x,t)]^2}\frac{\partial c(x,t)}{\partial x} + \frac{v_0}{1+c(x,t)}c(x,t) \tag{13}$$

i.e. the density current is the sum of a *diffusive* and a *convective* term. It contains the coefficient of collective or chemical diffusion,

$$D[c(x,t)] = \frac{D_0}{[1+c(x,t)]^2} \tag{14}$$

and the mean particle velocity

$$v[c(x,t)] = \frac{v_0}{1+c(x,t)}\,. \tag{15}$$

Note that the diffusion coefficient and the mean particle velocity depend on the instantaneous values of the concentrations. Again, in equilibrium the static solution of (12) is given by Bose distribution.

Equations (12) and (13) are consequences of the assumption (11). However, the validity of this assumption must be examined. Equation (12) (the *generalized* Burgers equation [6]) is transformed below to a form more proper for further applications.

Since we study diffusion near to equilibrium as well as near the stationary state, we split the concentration into $c(x, t) = \bar{c} + \delta c(x, t)$, and expand (12) and (13) around $\bar{c}$ up to quadratic order to obtain

$$\begin{aligned}\frac{\partial \delta c(x,t)}{\partial t} = &-\frac{v_0}{(1+\bar{c})^2}\frac{\partial \delta c(x,t)}{\partial x} + \frac{D_0}{(1+\bar{c})^2}\frac{\partial^2 \delta c(x,t)}{\partial x^2} \\ &+\frac{2v_0}{(1+\bar{c})^3}\delta c(x,t)\frac{\partial \delta c(x,t)}{\partial x} - \frac{2D_0}{(1+\bar{c})^3}\frac{\partial}{\partial x}\left[\delta c(x,t)\frac{\partial \delta c(x,t)}{\partial x}\right].\end{aligned} \tag{16}$$

The first line of (16) represents the linear approximation which is expected to cover an intermediate range of times. The second line contains the convective and another nonlinear term. Usually, the first term on the right-hand side of (16) is removed by a Galilei transformation to the co-moving frame. The Monte Carlo simulations are carried out in a fixed frame of reference relative to which the particles move.

In the linear part of the equation we can identify

$$D(\bar{c}) = \frac{D_0}{(1+\bar{c})^2} \tag{17}$$

as a collective or chemical diffusion coefficient, and

$$v(\bar{c}) = \frac{v_0}{(1+\bar{c})^2} \tag{18}$$

as a drift velocity of concentration fluctuations. The meaning of this velocity will be discussed further below. Here, the collective diffusion coefficient depends on concentration, whereas for the non-interacting fermionic lattice-gas [7–10] it is independent of concentration both in the presence and absence of a bias.

As discussed below, the nonlinearities resulting from the expansion of the diffusive term in (12) and (13) are *irrelevant* compared to the convective term. Hence, the fourth term in (16) can be neglected and we obtain the well known Burgers equation [6] with coefficients that are non-trivially dependent on average particle concentration.

In this derivation we did not but we could trace fluctuations. As usual in fluctuating hydrodynamics, we complete the Burgers equation by adding a Langevin force, which conserves particle number. The resulting model has been studied during the last decade in great detail (see e.g. [6, 9, 11] and references therein). For $v_0 \neq 0$, i.e. in the presence of a bias, the convective nonlinearity has been shown to cause a superdiffusive behaviour $t^{2/3}$-law for the RMS-displacement, in one dimension, in contrast to the usual diffusive $t^{1/2}$-law [9]. The fluctuating Burgers equation is equivalent to the KPZ equation for the height variable $h(x, t)$ in a class of growing-interface models (the condsidered quantities are related by $c(x, t) = \partial h/\partial x$) [11]. There, the superdiffusive behaviour corresponds to anomalous surface roughening and the asymptotic scaling laws have been derived from renormalized perturbation theory [11]. From dimensionality arguments (power counting), it is already clear that the diffusive nonlinearities (fourth term in (16)) are irrelevant. This is confirmed in the renormalization treatment below two dimensions.

In the case without bias the diffusive nonlinearities (fourth term in (16)) become relevant below four dimensions. We have not considered their possible influence analytically. From the simulations there is now evidence for their importance on the space and time scales considered here.

Sections 4 and 5 will show how well the results of the numerical simulations are described by the analytical results derived above.

4. Diffusion without drift

4.1. Collective diffusion

In this subsection we investigate collective diffusion in the one-dimensional bosonic lattice gas in the case $\Gamma_{\rightarrow} = \Gamma_{\leftarrow}$. Then the equilibrium state of constant overall density exists for the periodic boundary conditions which we use, but there appear fluctuations in the density of particles in finite regions of the system. These fluctuations decay according to Fick's law, and the corresponding diffusion coefficient is the one for collective or chemical diffusion. It is most directly studied by monitoring the decay of density profiles which are superimposed on the average density. This procedure was first implemented by one of the authors [8] (see [5] for a review). A slight extension of the original procedure as well as the details of our simulations are listed below.

In the simulations, we prepare the system with the initial condition

$$\delta c(l, 0) = \Delta c(0) \cos[k(l - l_{\text{shift}})] \tag{19}$$

and choose $\Delta c(0) = 0.1$, i.e. always distinctly smaller than the average concentrations. The time dependence of the concentration profile $\delta c(l, t)$ is *monitored* and *fitted* by

$$\delta c(l, t) = \Delta c(t) \cos[k(l - l_{\text{shift}})]\,. \tag{20}$$

In the long-wavelength limit, the coefficient $\Delta c(t)$ of this Fourier component is a solution of the linearized diffusion equation

$$\Delta c(t) = \Delta c(0) \exp\left[-D(\bar{c})k^2 t\right] \tag{21}$$

and hence we can determine the coefficient of collective diffusion, $D(\bar{c})$.

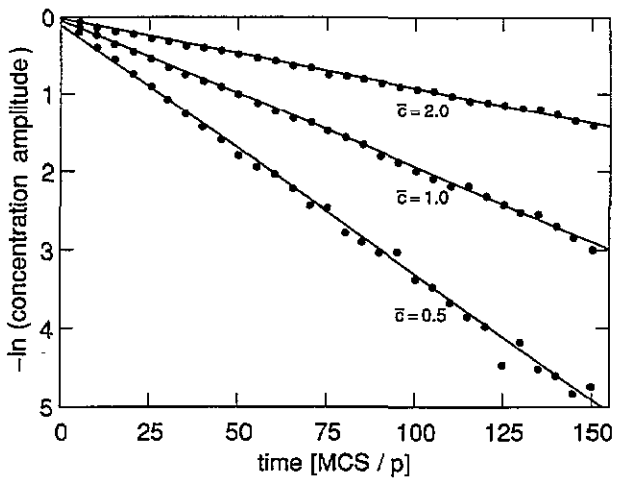

Figure 2. Amplitudes of concentration profile in a semilogarithmic plot versus Monte Carlo steps per particle for the bosonic lattice gas in the absence of a bias. Full circles denote results of Monte Carlo simulations for three different concentrations: $\bar{c} = 0.5$, 1.0 and 2.0, respectively; the full curves represent fits with (21).

The only extension compared to the original method is the shift parameter l_{shift} (in our calculations equal to $\frac{1}{2}$) chosen so that the nodes of the immobilized wavy particle concentration profile (given by (20)) and the lattice sites to make incommensurable. By this step, the zeros of the denominator are located between the lattice sites and therefore improved 'experimental' statistics for $\delta c(l, t)$ is achieved numerically. Also, the periodic boundary conditions are not affected by this approach; note that we used a reasonably small wavevector, i.e. $k = 2\pi/\lambda = 0.3927$, where $\lambda = 16$, and the chains had $2^{15} (= 32768)$ sites.

Figure 2 shows the decay of the concentration profile for three typical equilibrium concentrations as a function of time in a semilogarithmic plot. The long-time behaviour is well described by straight lines, except for some scattering of the data points for small amplitudes. The initial-time decay is slightly enhanced, but this is likely to be an artefact of the initial preparation. We also examined the wavelength dependence of the results (the rate of the exponential decay scales as $k^2 = (2\pi/\lambda)^2$), and the absence of nonlinear effects within the accuracy of the numerical simulations. The diffusion coefficients deduced from the slopes of figure 2 agree with the collective diffusion coefficient $D(\bar{c})$ as given by (17), within a few per cent. Hence the simulations verify the validity of the linearized version of (16) for the diffusive decay of small deviations from the equilibrium concentrations.

4.2. Centre-of-mass diffusion

In this subsection we examine numerically an asymptotic formula for the mean-square displacement of the centre of mass as a function of time. The starting point is a general asymptotic formula in the long-wave approximation [9, 10], which relates the centre-of-mass mean-square displacement with a time-dependent density–density correlation function

$$\langle [X(t)]^2 \rangle N_p = \frac{2}{N\bar{c}} \lim_{k \to \infty} \left[\frac{S(k, 0) - S(k, t)}{k^2} \right]. \tag{22}$$

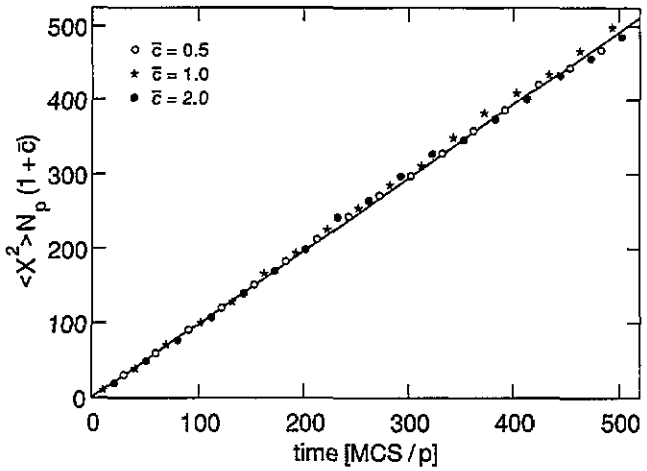

Figure 3. Scaled centre-of-mass mean-square displacement versus Monte Carlo steps per particle. Empty circles, stars, and full circles denote results of Monte Carlo simulations for three typical concentrations: $\bar{c} = 0.5$, 1.0, 2.0, respectively, without bias. The full line represents the theory discussed in section 4.2.

The time-dependent centre-of-mass displacement is defined as $X(t) = 1/N_p \sum_{j=1}^{N_p} \Delta x_j(t)$, where $\Delta x_j(t)$, $j = 1, \ldots, N_p$, is the displacement of the jth particle at time t, and $S(k,t) = \langle \tilde{\delta}c(-k,0)\tilde{\delta}c(k,t)\rangle$ is the density–density correlation function with $\tilde{\delta}c(k,t)$ the spatial Fourier transform of a concentration fluctuation $\delta c(x,t)$. When the linearized diffusion equation holds

$$S(k,t) = S(k,0)\exp[-k^2 D(\bar{c})t] \tag{23}$$

and the equal-time density fluctuations $S(k,0)$ are easily related, in the grand-canonical ensemble, to the fluctuations of the particle number N_p in the bosonic lattice gas

$$\lim_{k\to 0} S(k,0) = \langle N_p^2\rangle - \langle N_p\rangle^2 = N\bar{c}(1+\bar{c})\,. \tag{24}$$

Using (23) and (24) we obtain finally the relation

$$\langle [X(t)]^2\rangle N_p = 2(1+\bar{c})D(\bar{c})t\,. \tag{25}$$

One may directly define a centre-of-mass diffusion coefficient by $D_{CM} = (1+\bar{c})D(\bar{c})$. By virtue of (17) it is given by

$$D_{CM} = \frac{D_0}{1+\bar{c}}\,. \tag{26}$$

In figure 3 we present results of Monte Carlo simulations for three typical concentrations. As is seen, they agree quite well with the above theoretical considerations, again verifying (17). Moreover, we emphasize that these results show the absence of nonlinear effects, within the accuracy of the numerical simulations and within the time range studied.

4.3. Tagged-particle diffusion

The diffusion of tagged particles in the one-dimensional model of a bosonic lattice gas with order preservation is interesting in several aspects. In the fermionic lattice gas with site exclusion, the mean-square displacement of tagged particles is characterized by an

asymptotic $t^{1/2}$ behaviour, instead of the usual proportionality with t. This subdiffusive behaviour is a consequence of the fact that the particles cannot pass each other on the chain. Here we have the *same constraint* and can expect a similar behaviour.

A physical derivation of the $t^{1/2}$ behaviour was given by Alexander and Pincus [12]. They pointed out that the fluctuations of the positions of tagged particles are driven by the density fluctuations of the particles, which decay by collective diffusion. In [12] the average mean-square displacement of a tagged particle has been related to the time-dependent density–density correlation function. For the bosonic lattice gas (as well as for the fermionic lattice gas) the equal-time density fluctuations are easily calculated in the grand-canonical ensemble (cf section 4.2). The decay is governed, in the hydrodynamic limit, by the coefficient of collective diffusion as given by (17). Using these modifications in the derivation of Alexander and Pincus, one obtains for the mean-square displacement of a tagged particle

$$\langle [x(t) - x(0)]^2 \rangle = 2\frac{1+\bar{c}}{\bar{c}}\sqrt{\frac{D(\bar{c})}{\pi}}t\,. \tag{27}$$

(Note that the lattice constant has been set to unity.)

The mean-square displacement of tagged particles is easily estimated by simulations. One considers each particle as tagged and monitors their displacements. The results for three particle concentrations are shown in figure 4. One observes that the simulation data approach the theoretical curves in the long-time limit. As for the fermionic lattice gas cf [13] the crossover to the asymptotic behaviour occurs earlier for larger concentrations. A fit with the data points to a power-law behaviour with an undetermined exponent and the prefactor confirms the validity of (27). Apart from its intrinsic interest, the results for the tagged-particle diffusion corroborate the validity of (17) for the coefficient of collective diffusion.

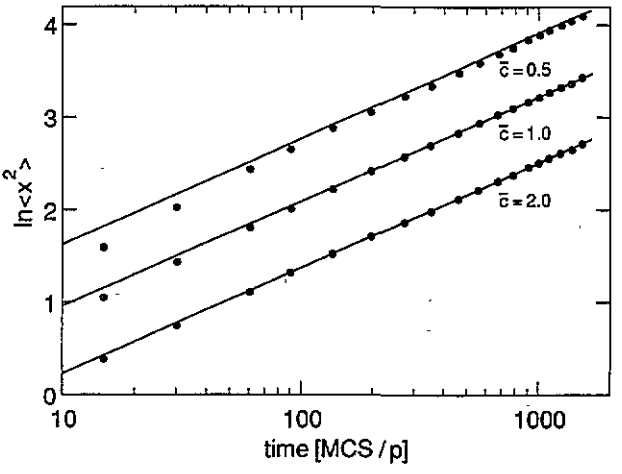

Figure 4. Mean-square displacement of the tracer particles versus Monte Carlo steps per particle in a double-logarithmic presentation. Full circles represent the results of Monte Carlo simulations for three typical concentrations, without bias, and the full lines represent the theory discussed in section 4.3.

5. Diffusion in the presence of drift

5.1. Centre-of-mass velocity

As a first step of this subsection we derive the equation of motion for the mean displacement of the centre-of-mass starting from (6) for the concentration $c(l,t)$. Multiplying both sides of this equation by l and summing over l we get as an intermediate step the *exact* equation for an infinite chain:

$$\frac{\mathrm{d}\langle X(t)\rangle}{\mathrm{d}t} = (\Gamma_{\rightarrow} - \Gamma_{\leftarrow}) \lim_{N\to\infty} \frac{1}{N_p} \sum_l P(l,t) \tag{28}$$

with the mean centre-of-mass displacement $\langle X(t)\rangle = \sum_l l[c(l,t) - c(l,0)]$; this definition is equivalent to that introduced in section 4.2.

Applying assumption (11) to the RHS of above equation and expanding it around $\bar{c}$, we obtain the final equation up to the second order in $\delta c(l,t)$ in the form

$$\frac{\mathrm{d}\langle X(t)\rangle}{\mathrm{d}t} = (\Gamma_{\rightarrow} - \Gamma_{\leftarrow}) \frac{1}{1+\bar{c}} \left\{ 1 + \frac{1}{N_p} \frac{\bar{c}}{(1+\bar{c})^2} \sum_l [\delta c(l,t)]^2 \right\}. \tag{29}$$

The second term in the braces is only a higher-order correction (of one per cent order) in our simulations, since we always keep $|\delta c(l,t)| \ll \bar{c}$. Hence we have in the lowest approximation the following formula for the centre-of-mass drift velocity:

$$v_{\mathrm{CM}}(\bar{c}) = \frac{\Gamma_{\rightarrow} - \Gamma_{\leftarrow}}{1+\bar{c}}. \tag{30}$$

We introduce the probability of jumps to the right as the parameter that characterizes the bias

$$p = \frac{\Gamma_{\rightarrow}}{\Gamma_{\rightarrow} + \Gamma_{\leftarrow}}. \tag{31}$$

Figure 5 allows us to examine relation (30) for three typical average concentrations at three different values of the bias. Again, the absence of nonlinear effects is clearly seen

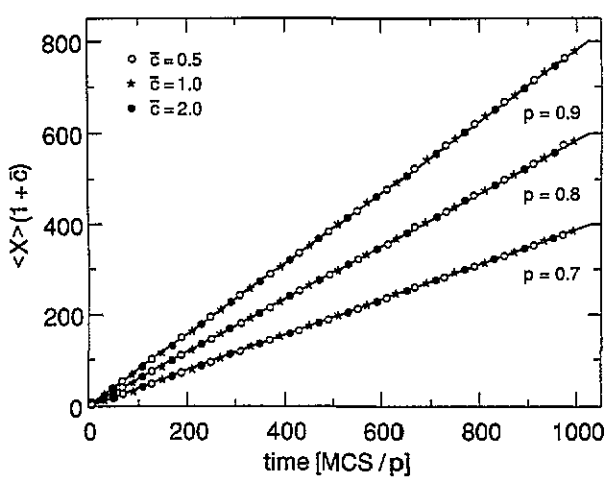

Figure 5. Scaled centre-of-mass displacement versus Monte Carlo steps per particle for three values of the bias $p = 0.7$, 0.8 and 0.9. Open circles, stars and full circles represent the data obtained by the Monte Carlo simulations for three typical concentrations. The full lines represent the theoretical results discussed in section 5.1.

within the accuracy of the numerical simulation and within the time range studied. Note that the centre-of-mass velocity has a different concentration dependence than the drift velocity which was introduced in the context of the Burgers equation (cf (18)). We will discuss the latter velocity in the following subsection and in the conclusion.

5.2. Drift velocity

Here we extend the method used in section 4.1 to directly verify (18). A solution of the linear part of (16) which represents a travelling wave is easily obtained in the long-wavelength limit

$$\delta c(l,t) = \Delta c(t)\cos[kl - v(\bar{c})t] \tag{32}$$

where $v(\bar{c})$ is the velocity which appears in (18). The coefficient $\Delta c(t)$ is again given by the solution of the linearized diffusion equation, i.e. by (21). In contrast to (19) and (20), we have set $l_{\text{shift}} = 0$ since the velocity already provides a time-dependent shift. The initial conditions are the same as in the case of no bias. The results of this approach are shown in figures 6 and 7.

Figures 6(*a*)–(*c*) present typical snapshot pictures showing scaled profiles $\delta c(l,t)/\Delta c(t)$ at three different times which travel to the right according to the external bias. The full circles represent data of the Monte Carlo simulation while the full curve represents the fit of these data by the weighted cosine, $g\cos[k(l - l(t))]$, where the amplitude g and the phase shift $l(t)$ are free parameters. If the linear version of (16) would be an exact diffusion equation of the bosonic lattice gas then the amplitude would be exactly $g = 1$, independently of time. Remember that the diffusive decay of the profile is taken into account in the linear approximation by the scaling with $\Delta c(t)$. From figure 6 we see that a slight decrease of the amplitude of the order of a few per cent occurs, which probably is an artefact due to the initial preparation.

The phase shift, $l(t)$, is time-dependent and numerical values taken from the fit are presented in figure 7 after scaling with the factor $(1 + \bar{c})^2$, for three typical concentrations and two values of the bias. As is seen, these numerical results agree with the theoretical prediction of (18) only up to about 10 Monte Carlo steps per particle (MCS/p); for longer times and, especially, for higher values of the bias clear deviations from the linear behaviour are seen. These data when properly evaluated could provide information of the influence of nonlinear corrections. We will follow a different (more tried) route to study their influence.

5.3. Centre-of-mass superdiffusion

In earlier papers [9, 10] that dealt with the fermionic lattice gas, an asymptotic formula for the dispersion of the centre-of-mass displacement was derived analytically by employing, in the simplest approximation, a *mode-coupling* formalism, and also verified numerically by one of the authors [10]. The reformulation of this derivation for the bosonic lattice gas, described by (16) with neglected diffusive nonlinearity (fourth term), is straightforward and gives

$$\left\{\left\langle [X(t)]^2\right\rangle - \langle X(t)\rangle^2\right\} N_{\text{p}} \approx 2D_{\text{CM}}(\bar{c})t + E(p,\bar{c})t^{4/3}\,. \tag{33}$$

In this formula we can clearly distinguish between the diffusion term which is linear in time and the nonlinear superdiffusive term. For the linear term the derivation yields $D_{\text{CM}}(\bar{c}) = (1 + \bar{c})D(\bar{c})$, i.e. (26) is equally valid in the equilibrium and in the stationary state. The *superdiffusion* coefficient is $E(p,\bar{c}) = (9/2\sqrt{\pi})^{2/3} D_{\text{CM}}(\bar{c})\gamma(p,\bar{c})^{1/3}$, with $\gamma(p,\bar{c}) = [(2p-1)^2\bar{c}/(1+\bar{c})^2]^2$.

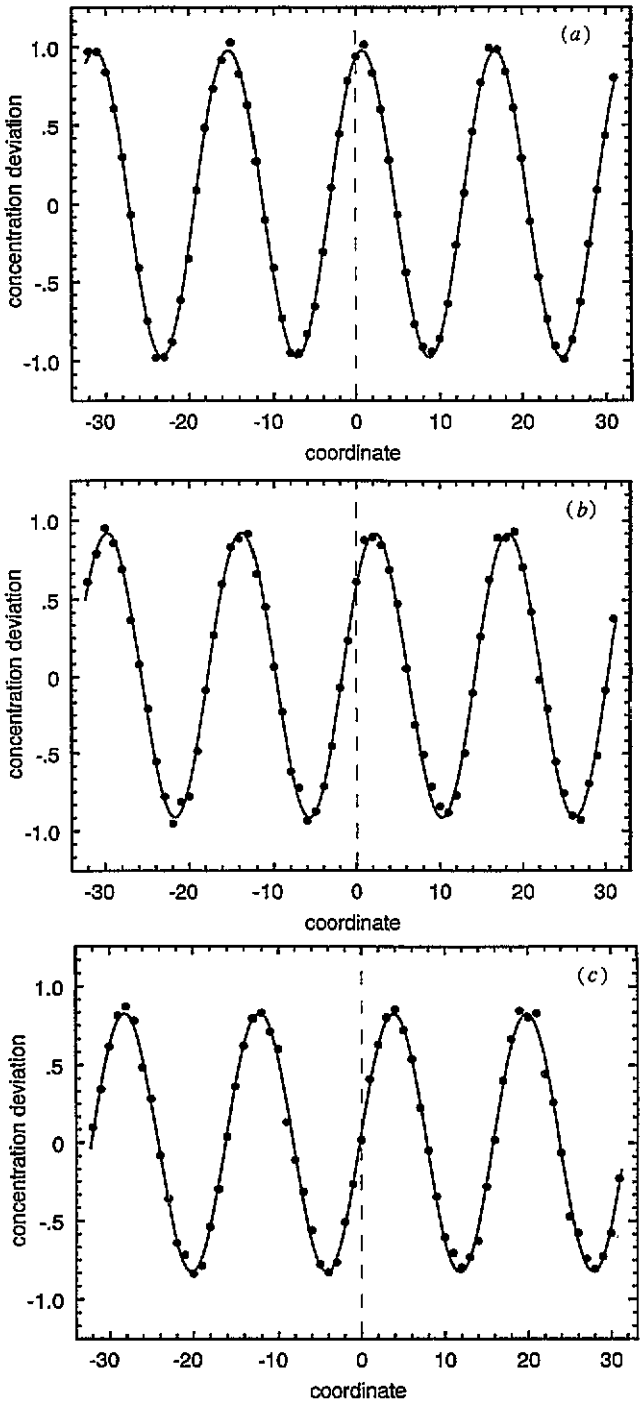

Figure 6. Snapshot picture of scaled deviation of concentration $(\delta c(l,t)/\Delta c(t))$ versus the x-coordinate for three moments of time: (a) $t = 3$ MCS/p, (b) $t = 9$ MCS/p and (c) $t = 18$ MCS/p, at $\bar{c} = 1.0$ and $p = 0.9$. The full circles represent the Monte Carlo data while the full curve is a fit to (32).

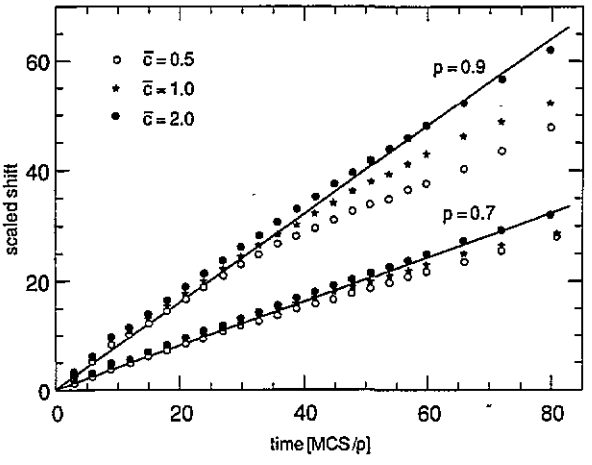

Figure 7. Scaled phase shift, $l(t)$, versus time for two values of the bias and three typical concentrations. Symbols, Monte Carlo simulations; full lines, linear theory $[(1+\bar{c})^2 v(\bar{c})t = (2p-1)t]$.

In the case of no bias ($p = \frac{1}{2}$) the superdiffusion term vanishes; however, when bias is present the diffusive term is still visible on a shorter time scale:

$$t \ll \frac{2}{\pi}\left\{(1+\bar{c})^2/\left[9\bar{c}(p-1/2)^2\right]\right\}^2 \tag{34}$$

which is obtained from (33) by comparing the diffusion and the superdiffusion term. For our parameter values this criterion says that for a time range not larger than a few MCS/p, the diffusion term dominates strongly, while for larger times superdiffusion almost totally dominates diffusion. This is demonstrated in figure 8 where data are given for the short-time behaviour of the dispersion of the centre-of-mass displacement for typical concentrations and an intermediate value of the bias.

Figure 9 shows the dispersion of the centre-of-mass mean displacement for one particular value of the bias and concentration on a more extended time scale. One recognizes the systematic behaviour $\sim t^{4/3}$, but also some regular oscillations around the systematic behaviour, which will be discussed in the following subsection. In table 1 we compare numerical and theoretical values of the superdiffusion coefficient for three values of p and a typical value of $\bar{c}$. The agreement is within about 20%. This is somewhat larger but comparable to the deviation found for the fermionic lattice gas [9]. Part of the discrepancy might be due to the fact that the numerical prefactor of $E(p,\bar{c})$ comes from an approximate solution of the integro-differential equation for the scaling function in [9]. On the other hand,

Table 1. Comparison of theoretical and numerical values of the superdiffusion coefficient at $\bar{c} = 1.02$.

p	$(1+\bar{c})tE(p,\bar{c})$	
	Simulation	Theory
0.69	0.256	0.203
0.85	0.528	0.459
1.0	0.627	0.739

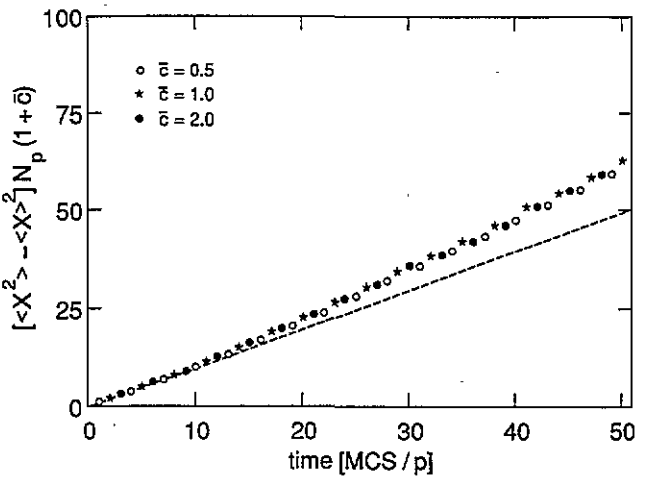

Figure 8. Typical initial behaviour of the scaled centre-of-mass mean-square displacement (with subtracted drift) versus Monte Carlo steps per particle in presence of a bias ($p = 0.7$). Open circles, stars and full circles are the Monte Carlo results for typical concentrations, and the broken line is the theoretical prediction for shorter times discussed in section 5.

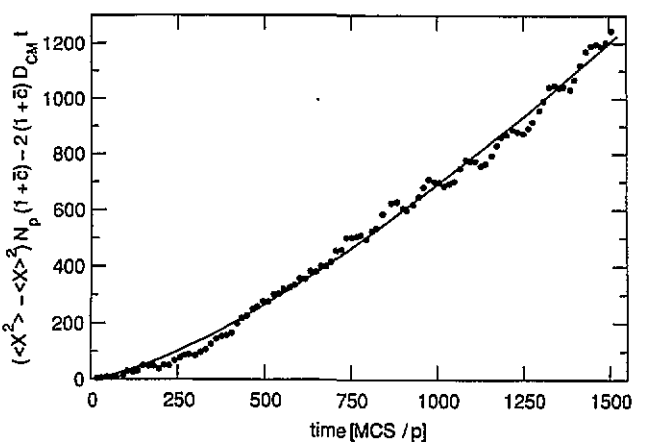

Figure 9. Dispersion of centre-of-mass displacement versus Monte Carlo steps per particle, for the bias $p = 0.65$ and the concentration $\bar{c} = 2.0$. Full circles represent the Monte Carlo data, and the full curve is the fit to a $t^{4/3}$ behaviour. The presence of oscillations is seen at larger times.

the deviation changes sign when approaching the largest value of driving force ($p = 1$). This could be understood from the fact that the mode-coupling approximation applies for small coupling constants only. The crossover in amplitudes to the strong coupling limit has been explored in [14]. This could lead to a saturation in the amplitude. However, the strong coupling problem is still unsolved in finite dimensions (see e.g. [15]).

One may introduce an effective exponent $\alpha(p)$ for the superdiffusive behaviour when the dispersion of the centre-of-mass displacement is fitted to a power-law behaviour $\sim t^{\alpha(p)}$ on an intermediate time scale. When the bias parameter is continuously increased from $p = \frac{1}{2}$ to larger values, the effective exponent should change from $\alpha = 1$ (normal diffusion)

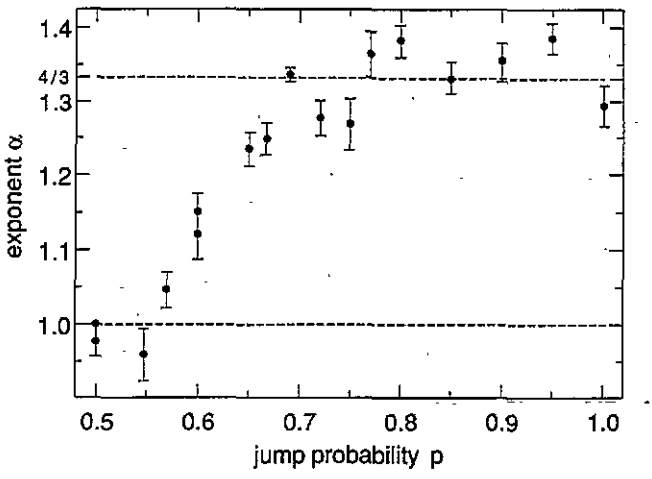

Figure 10. The effective superdiffusion exponent α versus bias p, changing continuously from $\alpha = 1$, for the case of no bias, toward $\alpha = \frac{4}{3}$, in the presence of a bias.

to $\alpha = \frac{4}{3}$ (superdiffusion). We have observed such a behaviour in our data, and figure 10 shows the results of this analysis.

5.4. Anomalous slow cluster dynamics

Figure 9 exhibited some regular oscillations around the systematic behaviour $\sim t^{4/3}$, with non-increasing amplitude. In this subsection we argue that this, oscillatory behaviour is likely due to a slowing-down effect of the dynamics of clusters for one particular combination of the parameters p and $\bar{c}$. We call an accumulation of $m > 1$ particles at a site l and we consider a cluster of the particles at this site. If there is bias in the positive direction, there is drift of the particles in this direction. Clusters with particle numbers above the average density will systematically decay in both directions. We direct the attention to the decay of the cluster by processes in the opposite direction to the bias. That is, we require that the top particle of the cluster (cf figure 1) does not make a transition. The cluster may decay by transition of the particle occupying the bottom of the cluster to site $l-1$, and the corresponding rate is $1/(1+\bar{c})\Gamma_{\leftarrow}$, where the factor $1/(1+\bar{c})$ represents the average probability of finding a vacancy at a given site (here at the bottom of the cluster). It may grow by transitions from site $l-1$. The growth rate is given by $\bar{c}/(1+\bar{c})^2\Gamma_{\rightarrow}$, where the factor $\bar{c}/(1+\bar{c})^2$ represents the average probability of finding at least one particle at site $l-1$, and having the jumping particle at the top of this cluster, cf (8). The dynamics of the cluster becomes particularly slow when growth and decay compensate each other on the average, or

$$\frac{\bar{c}}{1+\bar{c}}\Gamma_{\rightarrow} = \Gamma_{\leftarrow}. \tag{35}$$

Introduction of the probability p of jumps in the positive direction leads to the special value

$$p_s = \frac{1+\bar{c}}{1+2\bar{c}}. \tag{36}$$

For instance, $p_s = \frac{2}{3}$ for $\bar{c} = 1$. We observed *systematic* oscillations like the ones in figure 9 for combinations of p and $\bar{c}$ which are close to the value given by (36) and an absence of such oscillations for combinations that are further away from this value.

5.5. Biased tagged-particle diffusion and drift velocity

It is also interesting to study tagged-particle diffusion in the model in the presence of a bias. In the case of the fermionic lattice gas, tagged-particle diffusion becomes normal when a bias is present, i.e. the dispersion of the mean displacement of tagged particles increases linearly with time, for large times [16, 17]. The same behaviour is observed for our model of a bosonic lattice gas. Figure 11 presents the scaled mean-square displacement (with subtracted drift) versus Monte Carlo steps per particle, for three values of the bias and at three typical concentrations. As is seen, the results of the simulations are quite well described by straight lines that have slopes given by the $2D_{\rm tp}(\bar{c})(1+\bar{c})$, where the diffusion coefficient of tagged particles is

$$D_{\rm tp}(\bar{c}) = \frac{1}{2}\frac{\Gamma_{\rightarrow} - \Gamma_{\leftarrow}}{1+\bar{c}}. \tag{37}$$

This expression requires justification.

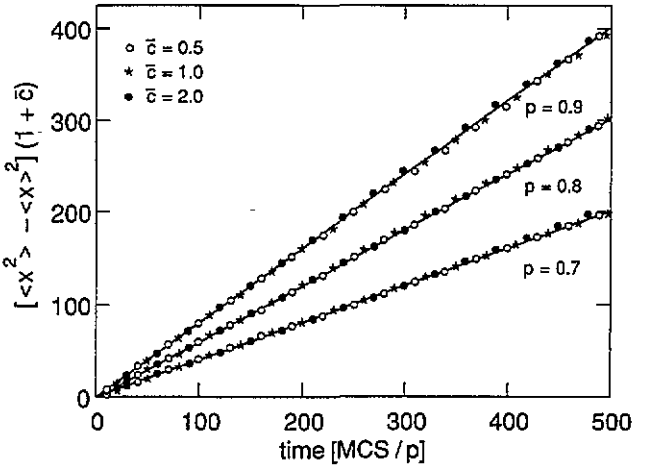

Figure 11. Scaled mean-square displacement of tagged particles with subtracted drift versus Monte Carlo steps per particle for the values of the bias $p = 0.7$, 0.8 and 0.9. Open circles, stars and full circles represent the Monte Carlo data for three typical concentrations. The full lines are the theoretical results discussed in section 5.5.

Recently, mathematicians derived [16] exact formulae for the tagged-particle diffusion coefficient and the drift velocity in the site-exclusion (fermionic) lattice gas. Their formalism can readily be extended to the model of a bosonic lattice gas, as a consequence of the requirement of order preservation, since then the same constraint applies in both models. In the fermionic lattice gas the basic local quantity is the effective jump rate $(1-\bar{c})\Gamma_j$ ($j = \rightarrow, \leftarrow$) of a tagged particle to the right or left nearest-neighbour site, where the factor $1-\bar{c}$ denotes the average probability of finding a vacancy at a given site. In the case of the bosonic lattice gas this factor should be replaced by $1/(1+\bar{c})$, according to (8). Then the rate $\Gamma_{\rightarrow}/(1+\bar{c})$ represents the transition rate of a particle occupying the top of the local cluster to the nearest-neighbour site. A similar interpretation applies to the jump rate $\Gamma_{\leftarrow}/(1+\bar{c})$ of a particle at the bottom of the local cluster to the left.

It is a matter of straightforward extension to also adopt a one-dimensional 'special vacancy' formalism developed earlier [13, 17] to derive the coefficient of tagged-particle diffusion and the mean drift velocity. We obtain the expression given in (37) for the tagged-

particle diffusion coefficient and the following expression for the drift velocity of tagged particles:

$$v_{tp} = \frac{\Gamma_{\rightarrow} - \Gamma_{\leftarrow}}{1 + \bar{c}}. \tag{38}$$

The mean drift velocity of tagged particles agrees with the velocity that follows from the mean displacement of the centre of mass, cf (30). In fact, the definitions of the mean displacement of the centre of mass, and of the displacement of tagged particles, averaged over all particles, are completely equivalent. As already stated above, our Monte Carlo simulations verify the validity of (37) for the diffusion coefficient of tagged particles.

6. Concluding remarks

In this paper we have discussed different types of diffusion in the one-dimensional bosonic lattice gas with order preservation, with and without bias:

- collective (or chemical) diffusion,
- centre-of-mass diffusion,
- tagged-particle diffusion.

We have studied linear and some aspects of nonlinear diffusion with non-trivial concentration-dependent diffusion coefficients and drift velocities. We observed both normal and anomalous diffusion in the model. In our studies, we 'experimentally' proved by Monte Carlo simulations that our basic hypothesis, i.e. relation (11) between $P(l, t)$ and $c(l, t)$, is valid not only near the equilibrium or stationary state but even far from them. We were able to verify, for example, the concentration dependence of different diffusion coefficients, drift velocities and superdiffusion coefficient of centre-of-mass dispersion.

It is instructive to compare the results for the different diffusional behaviours of the bosonic lattice gas in one dimension with the corresponding ones of the fermionic lattice gas. This is done in table 2. Of course, the different drift velocities are zero when no bias is present. Also, the coefficient of tagged-particle diffusion vanishes in the absence of a bias since then the mean-square displacements show subdiffusive behaviour.

The table demonstrates that the collective diffusion coefficient and the collective drift velocity are scaled by the factor $1/(1+\bar{c})$ in comparison to the analogous quantities for the centre-of-mass and tagged-particle diffusion.

Both models are completely equivalent *only* at $\bar{c} = 0$. At small but finite $\bar{c}$ the models are already *not* equivalent. Expanding the factor $1/(1+\bar{c})$ and $1/(1+\bar{c})^2$ up to first order, we observe that the equivalence between both models is broken only for collective (or

Table 2. Diffusion coefficients and drift velocities for the bosonic and fermionic lattice gases in the absence and presence of a bias. The different diffusion coefficients and velocities were defined in the main text. The sum of the transition rates $\Gamma_{\rightarrow} + \Gamma_{\leftarrow}$ and the lattice constant has been set to unity.

	$2D$	$2D_{CM}$	$2D_{tp}$	$v(\bar{c})$	$v_{CM} = v_{tp}$
No	$1/(1+\bar{c})^2$	$1/(1+\bar{c})$	0	0	0
bias	1	$1-\bar{c}$	0	0	0
Bias	$1/(1+\bar{c})^2$	$1/(1+\bar{c})$	$\frac{2p-1}{(1+\bar{c})}$	$\frac{2p-1}{(1+\bar{c})^2}$	$\frac{2p-1}{(1+\bar{c})}$
	1	$1-\bar{c}$	$(2p-1)(1-\bar{c})$	$(2p-1)(1-2\bar{c})$	$(2p-1)(1-\bar{c})$

chemical) diffusion without and with bias. Roughly speaking, this could be expected, since the possibility of *multiple* occupancy of sites for the bosonic lattice gas should modify just the collective diffusion. An additional reason for the broken equivalence is that there exists an *extra* symmetry for diffusion in the fermionic lattice gas (exhibited earlier [7, 10]) and *not* for diffusion in the bosonic one.

Acknowledgments

RK is grateful to Institut für Festköperforschung Jülich, Forschungszentrum Jülich, for the hospitality extended to him; RK also thanks Professor W Dieterich for discussion. This work was supported in part by the Polish KBN Grant no 2 P302 126 04, and by Deutsche Forschungsgemeinschaft, SFB 306.

References

[1] Przeniosło R, Barszczak T, Kutner R, Guzicki W and Renz W 1991 *Int. J. Mod. Phys.* C **2** 450
Przeniosło R, Andrzejewski M, Kwiatkowski M and Kutner R 1993 *Proc. 4th Int. Conf. on Physics Computing 1992* ed R de Groot and J Nadrchal (Singapore: World Scientific) p 450
[2] Rubinstein M 1987 *Phys. Rev. Lett.* **59** 1946
[3] Bouchaud J-P and Georges A 1990 *Phys. Rep.* **195** 127
[4] Barszczak T and Kutner R 1991 *J. Stat. Phys.* **62** 389
Kutner R and Barszczak T 1991 *J. Stat. Phys.* **65** 813
[5] Kehr K W and Binder K 1987 *Applications of the Monte Carlo Method in Statistical Physics (Topics in Current Physics 38)* ed K Binder (Berlin: Springer) p 181
[6] Burgers J M 1974 The nonlinear diffusion equation *Asymptotic Solutions and Statistical Problems* (Dordrecht: Reidel)
Boghosian B M and Levermore C D 1987 *Complex Systems* **1** 17
[7] Kutner R 1981 *Phys. Lett.* **81A** 239
[8] Kehr K W, Binder K and Reulein S M 1989 *Phys. Rev.* B **39** 4891
[9] van Beijeren H, Kutner R and Spohn H 1985 *Phys. Rev. Lett.* **54** 2026
Janssen H K and Schmittmann B 1986 Z. *Phys.* B **63** 517
Krug J 1987 *Phys. Rev.* A **36** 5465
[10] Kutner R and Bogusz W 1992 Z. *Phys.* B **86** 461
[11] Kardar M, Parisi G and Zhang Y C 1985 *Phys. Rev. Lett.* **56** 889
Medina E, Hwa T, Kardar M and Zhang Y-C 1989 *Phys. Rev.* A **39** 3053
Hwa T and Frey E 1991 *Phys. Rev.* A **44** R7873
Amar J G and Family F 1992 *Phys. Rev.* A **45** 5378
[12] Alexander S and Pincus P 1978 *Phys. Rev.* B **18** 2011 (The authors left out a factor $a/2\pi$ in their equation (4).)
[13] van Beijeren H, Kehr K W and Kutner R 1983 *Phys. Rev.* B **28** 5711
[14] Nattermann T and Renz W 1988 *Phys. Rev.* B **38** 5184
[15] Bouchaud J-P and Cates M E 1993 *Phys. Rev.* E **47** R1455
[16] De Masi A and Ferrari P A 1985 *J. Stat. Phys.* **38** 603
[17] Kutner R and van Beijeren H 1985 *J. Stat. Phys.* **39** 317